

Application of ATR–FTIR Spectroscopy Combined with Sputter Etching for Depth Profiling of a Chemical Additive within a Pulp Fiber

DAISUKE TATSUMI, TATSUO YAMAUCHI

Division of Forest and Biomaterials Science, Graduate School of Agriculture, Kyoto University, Kitashirakawa Oiwake-cho, Sakyo-ku, Kyoto 606-8502, Japan

Received 15 September 1997; accepted 23 November 1997

ABSTRACT: Attenuated total reflectance–Fourier transform infrared (ATR–FTIR) spectroscopy in combination with the sputter etching technique was applied to the determination of the depth distribution of a chemical additive within a pulp fiber. After etching successively, the surface additive content was determined by ATR–FTIR spectroscopy. Sputter etching until 5 min was homogeneous and proportional to obtain precise depth profile. From the relationship between etching time and the thickness of removed surface layer, it is possible to follow the partial concentration profiles of the additive as a function of distance from the original surface. The obtained profile is compared qualitatively with that of variable-angle ATR–FTIR depth profiling method. The profile shows that most of the additive is located at the fiber surface; however, some of it is broadly distributed toward the inside of the fiber. The present method can be used to clarify the distribution of other paper additives within a pulp fiber, and, moreover, it can be applied to depth profiling of a minor component within a solid material. © 1998 John Wiley & Sons, Inc. *J Appl Polym Sci* 69: 461–468, 1998

Key words: fibers; pulp additives; infrared spectroscopy; sputter etching; depth profiling

INTRODUCTION

The large majority of fibrous materials, including paper, contain chemical additives that play various functional roles. These additives can provide their function by spreading over or penetrating into the fibers. The amounts of them are too small to determine their quantities and their inter- and intrafiber distributions. In particular, it is hardly known how they are distributed within a fiber, although the properties of the fibrous materials may be largely affected by their distributions. We have previously reported that attenuated total reflectance–Fourier transform infrared (ATR–

FTIR) spectroscopy is useful for quantitative determination of a polyacrylamide resin (PAM), which is a dry-strength additive for paper sheets. It has been investigated from the band intensities of difference spectra obtained by spectral subtraction with a blank sheet spectrum.¹ This is the base to obtain a depth profile of PAM within a pulp fiber using ATR–FTIR spectroscopy.

ATR–FTIR spectroscopy has been widely applied to surface characterization of materials. Depth profiling with the use of ATR spectroscopy has been investigated by a variation in the penetration depth, d_p . It is defined as the depth at which the amplitude of the evanescent field decreases to $1/e$ of its value at the interface and is represented by²

$$d_p = \frac{\lambda}{2\pi(n_1^2 \sin^2 \theta - n_2^2)^{1/2}} \quad (1)$$

Correspondence to: D. Tatsumi.

Journal of Applied Polymer Science, Vol. 69, 461–468 (1998)
© 1998 John Wiley & Sons, Inc. CCC 0021-8995/98/030461-08

where λ is the wavelength of IR radiation, n_1 and n_2 are the refractive indices of the internal reflection element (IRE) and the sample, respectively, and θ is the angle of incidence. Several studies have been done to follow the extent of chemical changes in materials as a function of distance from the surface, assuming a function form for the unknown depth profile.^{3–5} To obtain quantitative depth profiles without an assumed function, the ATR intensities must be inverse-Laplace-transformed.⁶ Such an approach, however, may be limited because of the difficulty of numerical inversion of Laplace transformation.

In-depth profiling analysis, sectioning of the sample, and subsequent chemical analysis is the most direct and common technique.⁷ Instead of sectioning, surface etching such as sputtering is also commonly used. Sawatari⁸ has used X-ray photoelectron spectroscopy (XPS) for Ar⁺ ion-etched pulps in order to confirm the distribution of mesyl groups in the radial direction of the pulp fiber. As far as we know, however, ATR-IR analysis, in combination with the etching technique, has been used only to study the spectral changes associated with polymer morphology and the corresponding crystallinity features.^{9,10}

In this study, we first obtain a qualitative depth profile of the additive within a pulp fiber by the conventional angular-dependent ATR-FTIR measurement and then propose a novel ATR-FTIR analysis in combination with the sputter etching technique to describe the quantitative depth profile. In the latter method, the surfaces of pulp fibers are removed stepwise by sputter etching and then measured with ATR-FTIR. The uniformity of the sputter etching is also discussed.

EXPERIMENTAL

Materials

The pulp used for paper sheet making was a commercial bleached kraft pulp beaten to CSF 585 mL. A chemical additive used in this study was a cationic polyacrylamide resin (PAM), with an average molecular weight of 2×10^6 and a charge density of 0.6 meq/g, supplied from Arakawa Chemical Industries Ltd. (Osaka, Japan). An aqueous solution of the PAM was added to the pulp slurry in the range of 0.3–3.0%, based on dry pulp and dry polymer solids. A series of paper sheet was prepared according to the procedure described in a previous article.¹ The amount of

PAM retained in the sheets was determined by nitrogen analysis¹ prior to the following measurements.

Sputter Etching

The sample sheet cut in a rectangle of 40×14 mm was dried in vacuum for 24 h before etching. The sample on the electrode was sputter etched stepwise from 1 to 20 min in a radio frequency sputtering equipment Shinku Kiko RFS-200 under the following conditions: an electric power of 3 W, and an Argon gas pressure of 10 Pa.

Infrared Spectroscopy

ATR-FTIR spectra were collected on a Shimadzu FTIR-8200PC spectrophotometer (Shimadzu, Kyoto, Japan) equipped with a Shimadzu ATR-8000 attachment, with a KRS-5 or a Ge internal reflection element (IRE) of 45° facets ($50 \times 20 \times 2$ mm). Additionally, a Harrick ATR attachment mounted in a Bio-Rad FTS-60 spectrophotometer (Bio-Rad Laboratories, Digilab Division, Cambridge, MA) was used for the measurement with an incidence angle θ of 60°: the IRE was a Spectra-Tech KRS-5 or Ge 60° face angle 50-mm rhomboid (Spectra-Tech, Shelton, CT). Two pieces of paper sample (40×14 mm) conditioned at 23°C and 50% relative humidity were placed one on each side of the IRE. Pressure was then applied through elastic pads of rubber that placed at the back of the sample sheets in order to produce effective contact between the sample sheets and the IRE. The FT-IR data were collected over 100 single-beam scans with a resolution of 4 cm^{-1} . The penetration depths (d_p) imposed by the available reflection conditions in this investigation were calculated from eq. (1) and given in Table I based on an absorption wave number of 1670 cm^{-1} (C=O stretching attributable to Amide I of PAM¹¹).

For quantitative ATR measurement, polarized light should be used, but it decreases the intensity of the light; thus, it reduces the S/N level of the spectra obtained.¹² In the case of an isotropic sample and an incidence angle $\theta = 45^\circ$, the effect of nonpolarized light is negligible if the absorbance of a band is less than 0.5.¹³ Thus, polarized light was not used in the present study.

In order to isolate the selected band of PAM, difference spectra were obtained by spectral subtraction with a spectrum of a blank paper sheet.¹ The blank sheet was also etched for the same time as the sample sheet. Surface roughness of the pa-

per sheets has an effect on sample-IRE contact and further on the spectra; however, variations in sample-IRE contact can be corrected by internal normalization.¹ For internal normalization, the absorbance of the PAM characterizing band at 1670 cm^{-1} in a difference spectrum (ΔA_{PAM}) was divided by that of a reference band (A_{cell}), which is a characteristic cellulose band at 1319 cm^{-1} (assigned to CH_2 wagging¹⁴) in the sample spectrum; thus, the normalized absorbance ratio is $\Delta A_{\text{PAM}}/A_{\text{cell}}$. However, it is necessary to make a few corrections in the normalized values (see the Appendix).

Calculation of Surface PAM Content from Absorbance Ratio

An absorbance ratio gives the apparent surface content of chemicals.^{12,15} If a value R ($=\Delta A_{\text{PAM}}/A_{\text{cell}}$) is obtained for an ATR-FTIR spectrum of a sample sheet containing PAM, the apparent surface PAM content (C_{PAM}) should be given by¹²

$$C_{\text{PAM}}(\text{vol } \%) = [R/(R + R_0)] \times 100 \quad (2)$$

where R_0 is the relative absorbance ratio obtained by ATR-FTIR measurements on the pure materials of the components.¹² In this study, we used the ratio of A_{PAM} in Figure 1(A) to A_{cell} in Figure 1(B); they are the absorbances in ATR spectra of PAM film and cellulose film, respectively. The PAM film was prepared by solution casting of the polymer in water. The cellulose film was a commercially available cellophane that had been extracted twice in boiling water to remove plasticizer (glycerin). Although the spectrum of cellophane was somewhat different from that of paper due to the difference in their lattice type, the intensity of the band at 1319 cm^{-1} is affected to a very small extent by the structural change.^{16,17} A_{PAM} in Figure 1(A) was larger than 0.5, so it must be deviated from the true absorbance by the "nonpolarization" effect; therefore, it required some corrections.¹³ Then, we obtained the value $R_0 = 15.8$. C_{PAM} is expressed in a unit of cubical percentage (vol %),¹¹ which can be converted to mass percentage (wt %), as in the following equation:

$$C_{\text{PAM}}(\text{wt } \%) = \frac{1.3C_{\text{PAM}}(\text{vol } \%)}{1.3C_{\text{PAM}}(\text{vol } \%) + 1.5(100 - C_{\text{PAM}}(\text{vol } \%))} \times 100 \quad (3)$$

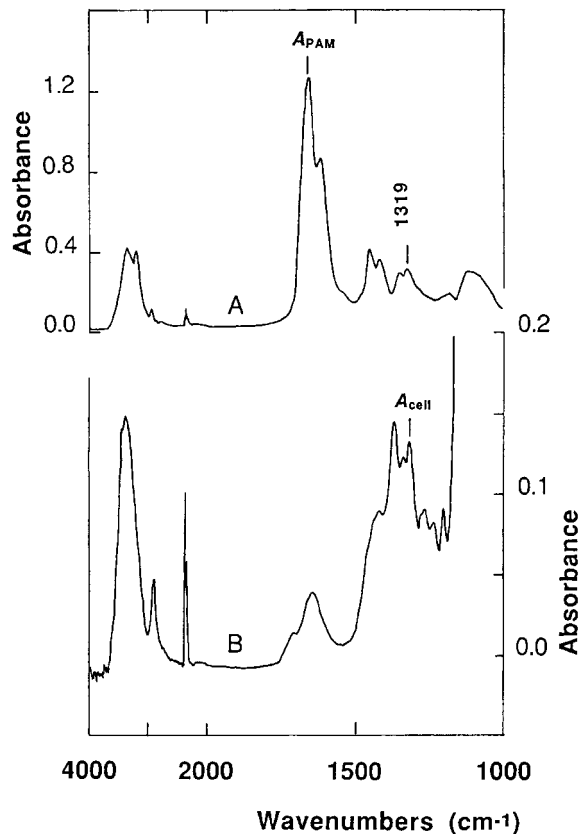


Figure 1 ATR spectra of PAM (A) cast film and (B) cellophane.

where the densities of PAM and pulp fiber were assumed 1.3 and 1.5 g/cm^3 , respectively.

RESULTS AND DISCUSSION

Depth Profiling by Variable-Angle ATR-FTIR Analysis

Paper sheets without etching were examined by ATR-FTIR analysis varying the penetration depth d_p . The apparent surface PAM contents (C_{PAM}) measured with 3 different penetration depths against the amounts of PAM retained in the sheets are shown in Figure 2. Since every C_{PAM} measured with $d_p = 1.2\text{ }\mu\text{m}$ (an ATR condition of KRS-5 IRE and $\theta = 45^\circ$, as shown in Table I) is close to the broken line, indicating bulk PAM content, the C_{PAM} with $d_p = 1.2\text{ }\mu\text{m}$ can be experimentally regarded as the bulk PAM content. This finding is reasonable, taking into consideration the fact that the d_p value is comparable to the fiber wall thickness (approximately $2\text{ }\mu\text{m}$ ¹⁸). Therefore, ATR-IR analysis with the specific ATR

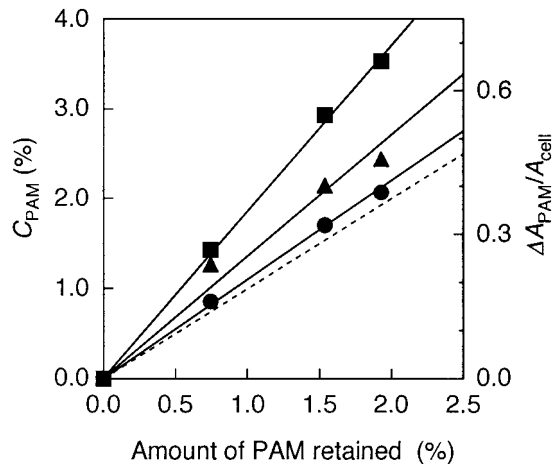


Figure 2 Apparent surface PAM content (C_{PAM}) versus amount of PAM retained in the sheets. Solid lines show the variation of C_{PAM} with penetration depths (d_p ; μm): (■) 0.40, (▲) 0.67, and (●) 1.2; broken line shows bulk PAM content.

condition ($d_p = 1.2 \mu\text{m}$) is regarded as a bulk analysis in the case of paper fibers.¹⁷

In each measuring case, C_{PAM} increases linearly with the amount of PAM retained in the sheet. The slopes of the lines become larger with decreasing d_p . It indicates that the additive exists very close to the fiber surface. This tendency is conveniently illustrated in Figure 3 by plotting C_{PAM} as a function of d_p at the PAM retained levels of 0.75 and 1.5%. The higher PAM content at smaller d_p indicates that PAM exists mainly at the fiber surface. However, these curves shown

Table I ATR Conditions and Penetration Depths (d_p) Calculated from Eq. (1)^a

IRE	n_1	Angle of Incidence (deg)		d_p (μm) ^d
		Nominal ^b	θ^c	
Ge	4.0	60	60	0.31
Ge	4.0	60	49	0.36
Ge	4.0	45	45	0.40
Ge	4.0	30	41	0.44
KRS-5	2.4	60	60	0.67
KRS-5	2.4	60	51	0.87
KRS-5	2.4	45	45	1.2

^a Refractive index of sample (n_2) is 1.5.

^b Not corrected for refraction at the entrance facet.

^c True angle corrected for refraction.

^d At 1670 cm^{-1} .

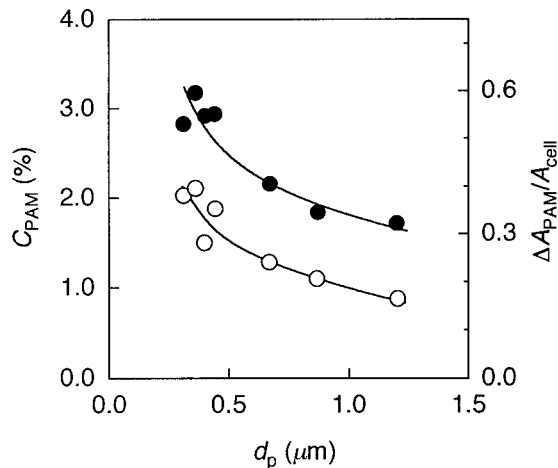


Figure 3 Variation in PAM content (C_{PAM}) with some penetration depths (d_p) at two levels of PAM retained in the sheets (%): (○) 0.75, and (●) 1.5.

in this figure are not simply related to the true concentration–depth profiles that exist across each fiber thickness because the observed $\Delta A_{\text{PAM}}/A_{\text{cell}}$ values depend on both the decreases of the IR electrical field amplitude and the fall off in the concentration of PAM, with increasing penetration into the fibers.³ Then we have examined a new ATR–FTIR analysis in combination with sputter etching.

Removal of Surface Layer by Sputter Etching

The overall process of sputter etching is surface erosion by the bombardment of primary particles (generally noble gas ions), which causes particles of the solid to be ejected from the surface. By continuous sputter etching, layers beneath the top-most layer are subsequently exposed.⁷

The etching rate was determined by measuring the weight loss of samples before and after sputter etching. Assuming that the sputter etching process operates uniformly, the thickness of etched layer Δz is given by

$$\Delta z = \frac{w - w'}{w} z \quad (4)$$

where w and w' are the weight of a sample before and after sputter etching, respectively, and z is the thickness of the sample before etching. Polyethylene terephthalate (PET) film and cellulose film (cellophane) were used for determination of the etching rate instead of paper samples. The thickness Δz linearly increased with etching time

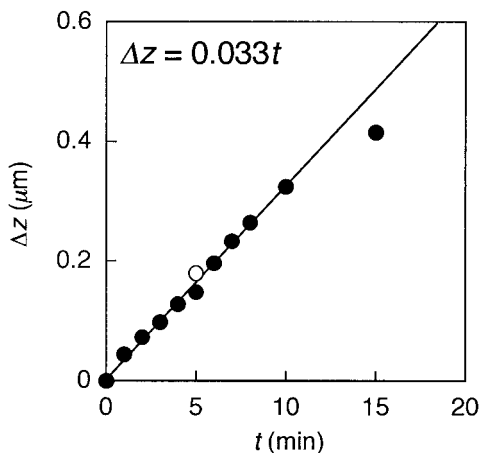


Figure 4 Experimental relationship between etching time (t) and thickness of etched layer (Δz) determined by mass decrease: (●) PET and (○) cellophane. Each spot is an average of 2–4 times measurement.

t for both films up to 10 min, as shown in Figure 4, and the calculated etching rate was 33 nm/min until 10 min for both films. Taking it into consideration that bleached pulp fibers almost consist of cellulose, the rate can be adopted for paper samples. Although the rate may be affected by the surface roughness of paper, it is negligible in the present study because the flat parts of the pulp fibers which make close contact with the IRE, are dealt with.

The etched surface was observed by a scanning electron microscope (SEM) to check uniform etching. Figure 5 shows the typical surface structure of the etched PET films. While no structural change was detected under 5 min etching, many rather homogeneous grain structures were emerged faintly through the entire film surface over 5 min of etching [Fig. 5(A); etched for 5 min], and the structures became larger by further treatment [Fig. 5(B); etched for 20 min]. Pulp

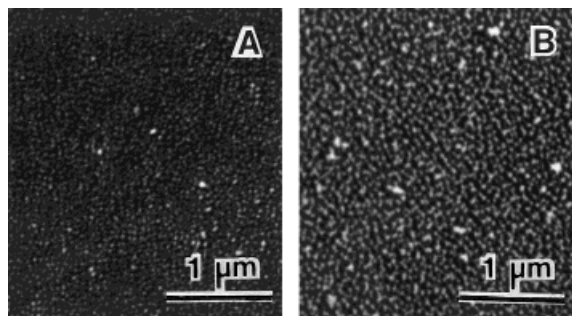


Figure 5 SEM images of etched PET films' surface: 5 (A) and 20 (B) min etching.

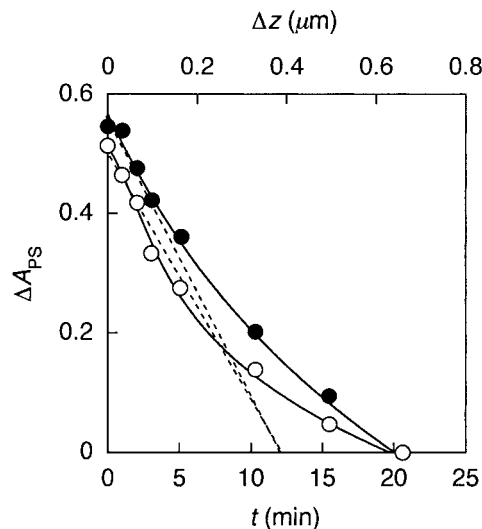


Figure 6 Absorbance of PS-coated PET film as a function of etching time (t). Broken lines show the proportional relation between absorbance and thickness of etched layer (Δz). IRE: (●) KRS-5 and (○) Ge, with a fixed angle $\theta = 45^\circ$.

fibers are also etched as the same manner as these films.¹⁹

The microstructure may affect the depth profiling of PAM within a paper fiber. Thus, a double-layered film, polystyrene (PS)-cast coated PET film, was etched stepwise and was then measured by ATR-FTIR in order to examine proportional etching. The original thickness of the coated PS film (z) was obtained by¹³

$$z = -\frac{d_p}{2} \ln \left[\frac{A_{\text{PET}}(z)}{A_{\text{PET}}(0)} \right] \quad (5)$$

where $A_{\text{PET}}(z)$ is an absorbance of a band (1345 cm^{-1} ; symmetrical methylene deformation²⁰) of PET, which is covered with PS layer of z thickness; thus, $A_{\text{PET}}(0)$ is the absorbance of uncovered PET. The thickness obtained was $0.39 \mu\text{m}$.

In the difference spectra of the double-layered film an aliphatic band²¹ at 1450 cm^{-1} was chosen for the standard band of PS. Absorbances of the band (ΔA_{PS}) were plotted against etching period in Figure 6, including the converted thickness of etched layer (Δz). Although the grain structures emerged by long time etching affect sample-IRE contact, errors caused by the incomplete contact can be corrected by the correction technique made by Ohta et al.¹¹ Each broken line represents an assumed absorbance if the sputter etching homogeneously removes PS layer with the etching rate

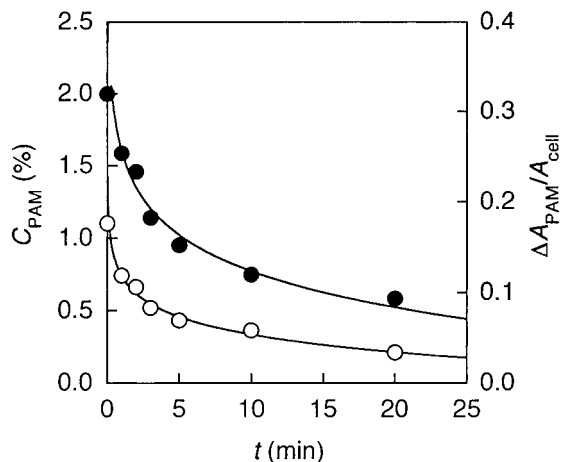


Figure 7 PAM content (C_{PAM}) as a function of etching time (t) at two levels of PAM retained in the sheets (%): (○) 0.75 and (●) 1.5.

(33 nm/min). The absorbances under homogeneous etching condition should linearly decrease with increasing etching time and diminish at 12 min of etching (that is, $\Delta z = 0.39 \mu\text{m}$), as shown by the broken lines. The observed absorbance ΔA_{PS} decreased along the assumed straight line with increasing etching time first, and then the decreasing rate is gradually reduced, regardless of different ATR conditions.

These results from Figures 4–6 prove that the etching until 5 min is homogeneous and proportional to obtain the precise depth profile. They further suggest that depth profiling over $0.2 \mu\text{m}$ needs some correction. The observed relationship between the absorbance and etching time in Figure 6 can be used for this purpose; Δz of 20 min etching sample was assumed to be the same as that of PS surface layer ($0.39 \mu\text{m}$).

Depth Profiling by ATR–FTIR Analysis with Sputter Etching

Surface removal by sputter etching and following ATR–FTIR measurement of the exposed surface was carried out successively for depth profiling. In Figure 7, the effect of sputter etching on the PAM content (C_{PAM}) measured with $d_p = 1.2 \mu\text{m}$ is shown, regarding it as bulk PAM content. C_{PAM} decreases logarithmically with increasing etching time. This is due to surface removal by sputter etching. Since the curved plots do not indicate actual concentration–depth profiles, a measured signal intensity versus sputtering time should be converted into a true concentration versus distance from the original surface.⁷

Now, $[C_{\text{PAM}}]_t$ and z_t are used for the apparent surface PAM content after t minutes of etching and the thickness of the etched layer during t minutes etching, respectively. The thickness z_t can be obtained from the calculated etching rate with some corrections described in the last section. Then we can obtain a value of $1 - [C_{\text{PAM}}]_t / [C_{\text{PAM}}]_0$; this means the contribution of the PAM content in the layer with a thickness of z_t to the bulk PAM content, assuming $[C_{\text{PAM}}]_0$ is the bulk PAM content. The contribution $(1 - [C_{\text{PAM}}]_t / [C_{\text{PAM}}]_0)$ is plotted against the thickness z_t (that is, the distance from the surface), as shown in Figure 8. The results show that the closer to the original surface, the larger is the contribution; for example, in the case of a PAM retained level of 0.75% a layer of $0.1 \mu\text{m}$ thickness from the original surface has a contribution of 0.5, while a layer of the same thickness at the depth from 0.2 to $0.3 \mu\text{m}$ has a contribution of 0.1. It shows that more than the half of the additive exists in a surface layer below $0.1 \mu\text{m}$ thickness.

In Figure 9 are shown differential distributions of each $0.1 \mu\text{m}$ of the curves in Figure 8. The ordinate was changed to PAM content (wt %) in each layer by multiplying each differentiated contribution by the bulk PAM content and a constant; the constant is the ratio of each layer thickness ($0.1 \mu\text{m}$) to fiber wall thickness (supposing $2 \mu\text{m}$ ¹⁸ in this study). This figure is considered to be the depth profiles of PAM within a fiber wall. It shows

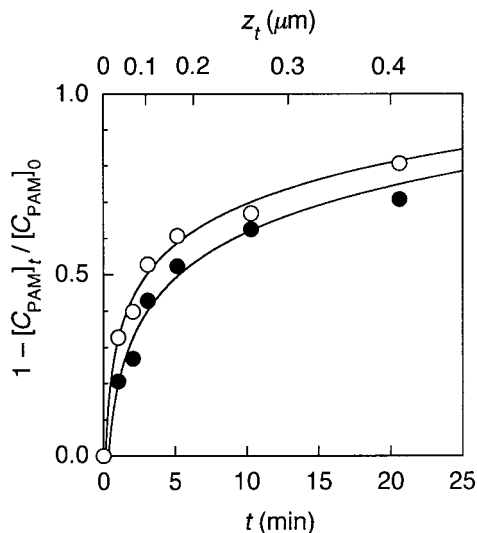


Figure 8 Dependence of the contributions $(1 - [C_{\text{PAM}}]_t / [C_{\text{PAM}}]_0)$ on etching time (t), which can be converted to distance from original surface (z_t). Legend is the same as in Figure 7.

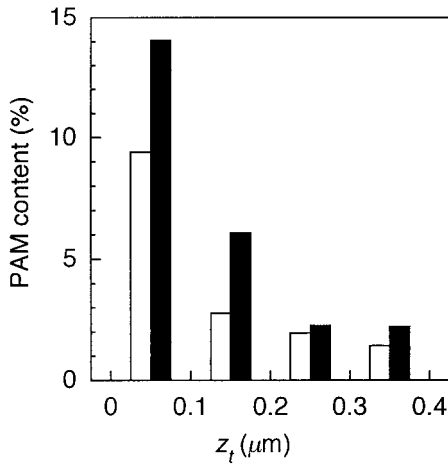


Figure 9 Depth profiles of PAM within a pulp fiber at two levels of PAM retained in the sheets (%): (□) 0.75 and (■) 1.5. This figure is based on the contribution curves in Figure 8.

that PAM content in the surface layer is very high. Most of the additive is located at the surface, and the content decreases toward inner side, regardless of the addition level. These results are compared favorably with those of the d_p -dependent ATR analysis.

CONCLUSIONS

ATR–FTIR spectroscopy in combination with the sputter etching technique has been applied to determination of the depth distribution of PAM within a pulp fiber. Assuming that the sputter etching process operates uniformly and that C_{PAM} measured with $d_p = 1.2 \mu\text{m}$ is comparable to the bulk PAM content, it is possible to obtain depth profiles of PAM within a fiber. The result has been found to be in reasonable agreement with those of the variable-angle ATR–FTIR analysis. The present method does not require an assuming function or complicated numerical inversion of Laplace transformation. This method can be used to clarify the distribution of other paper additives within a pulp fiber; and moreover, it can be applied to depth profiling of additives within a solid materials, as well as those in such fibrous materials.

The authors thank Arakawa Chemical Industries Ltd. for ATR–FTIR measurement with 60° facets IRE and for helpful suggestions.

APPENDIX: CORRECTION TECHNIQUE OF ABSORBANCE RATIO

When obtaining the difference spectrum, we adjusted the scale factor so that the reference band at 1319 cm^{-1} was appropriately canceled. However, the band intensity in the sample sheet spectrum should be stronger than that in the blank sheet spectrum because a band of PAM is overlapping with the reference band, A_{cell} . When the absorbance of the overlapping band is made to be ΔA_{over} , the absorbance at 1319 cm^{-1} in the sample sheet spectrum can be expressed by the sum of ΔA_{over} and A_{cell} . The spectral subtraction was done so that the absorbance at 1319 cm^{-1} in the sample sheet spectrum was adjusted to A_{cell} in the blank sheet spectrum with a scale factor $f (< 1)$ as follows:

$$A_{\text{cell}} = f(\Delta A_{\text{over}} + A_{\text{cell}}) \quad (\text{A.1})$$

Now the observed absorbance of the PAM characterizing band at 1670 cm^{-1} in the difference spectrum ($[\Delta A_{\text{PAM}}]_{\text{obs}}$) is given by the following equation including the factor f :

$$[\Delta A_{\text{PAM}}]_{\text{obs}} = f(\Delta A_{\text{PAM}} + A_{\text{blank}}) - A_{\text{blank}} \quad (\text{A.2})$$

where A_{blank} in the second term of the right side is the absorbance at 1670 cm^{-1} in the blank sheet spectrum, and then $f(\Delta A_{\text{PAM}} + A_{\text{blank}})$ represents the absorbance at the same wave number in the sample sheet spectrum. So the normalized absorbance ($[\Delta A_{\text{PAM}}/A_{\text{cell}}]_{\text{obs}}$) can be expressed as

$$\left[\frac{\Delta A_{\text{PAM}}}{A_{\text{cell}}} \right]_{\text{obs}} = \frac{f(\Delta A_{\text{PAM}} + A_{\text{blank}}) - A_{\text{blank}}}{A_{\text{cell}}} \quad (\text{A.3})$$

Then we can get the actual absorbance ratio ($\Delta A_{\text{PAM}}/A_{\text{cell}}$), as follows:

$$\begin{aligned} \frac{\Delta A_{\text{PAM}}}{A_{\text{cell}}} &= \frac{1}{f} \left\{ \left[\frac{\Delta A_{\text{PAM}}}{A_{\text{cell}}} \right]_{\text{obs}} + \frac{A_{\text{blank}}}{A_{\text{cell}}} \right\} - \frac{A_{\text{blank}}}{A_{\text{cell}}} \quad (\text{A.4}) \end{aligned}$$

Now let us consider that the absorbance of the overlapping band (ΔA_{over}) is $k (< 1)$ times as large as ΔA_{PAM} , as follows:

$$\Delta A_{\text{over}} = k \Delta A_{\text{PAM}} \quad (\text{A.5})$$

Then $1/f$ can be calculated from eqs. (A.1) and (A.5), as follows:

$$\frac{1}{f} = \frac{\Delta A_{\text{over}} + A_{\text{cell}}}{A_{\text{cell}}} = \frac{k\Delta A_{\text{PAM}}}{A_{\text{cell}}} + 1 \quad (\text{A.6})$$

Substitute eq. (A.6) into eq. (A.4) to eliminate the factor f , and let $\Delta A_{\text{PAM}}/A_{\text{cell}}$ be replaced by R , as follows:

$$R = (kR + 1) \left\{ \left[\frac{\Delta A_{\text{PAM}}}{A_{\text{cell}}} \right]_{\text{obs}} + \frac{A_{\text{blank}}}{A_{\text{cell}}} \right\} - \frac{A_{\text{blank}}}{A_{\text{cell}}} \quad (\text{A.7})$$

We have then

$$R = \frac{\left[\frac{\Delta A_{\text{PAM}}}{A_{\text{cell}}} \right]_{\text{obs}}}{1 - k \left(\left[\frac{\Delta A_{\text{PAM}}}{A_{\text{cell}}} \right]_{\text{obs}} + \frac{A_{\text{blank}}}{A_{\text{cell}}} \right)} \quad (\text{A.8})$$

where R is the corrected absorbance ratio. The factor k can be obtained from the ratio of the absorbance at 1319 cm^{-1} to A_{PAM} in the spectrum of PAM film [Fig. 1(A)]: $k = 0.110$.

REFERENCES

1. D. Tatsumi, T. Yamauchi, and K. Murakami, *Nord. Pulp Pap. Res. J.*, **10**, 94 (1995).

2. N. J. Harrick, *J. Opt. Soc. Am.*, **55**, 851 (1965).
3. D. J. Carlsson and D. M. Wiles, *J. Polym. Sci., Polym. Lett.*, **8**, 419 (1970).
4. D. J. Carlsson and D. M. Wiles, *Macromolecules*, **4**, 174 (1971).
5. H. G. Tompkins, *Appl. Spectrosc.*, **28**, 335 (1974).
6. T. Hirschfeld, *Appl. Spectrosc.*, **31**, 289 (1977).
7. S. Hofmann, *Surf. Interface Anal.*, **2**, 148 (1980).
8. A. Sawatari, *Mokuzai Gakkaishi*, **27**, 804 (1981).
9. H. A. Willis and V. J. I. Zichy, in *Polymer Surfaces*, D. T. Clark and W. J. Feast, Eds., Wiley, New York, 1978, Chap. 15.
10. J. A. Gardella Jr., J. S. Chen, J. H. Magill, and D. M. Hercules, *J. Am. Chem. Soc.*, **105**, 4536 (1983).
11. K. Ohta, R. Iwamoto, and M. Miya, *Nippon Kagaku Kaishi*, 1200 (1985).
12. R. Iwamoto and K. Ohta, *Appl. Spectrosc.*, **38**, 359 (1984).
13. K. Ohta and R. Iwamoto, *Appl. Spectrosc.*, **39**, 418 (1985).
14. C. Y. Liang and R. H. Marchessault, *J. Polym. Sci.*, **39**, 269 (1959).
15. J. M. G. Cowie, B. G. Devlin, and I. J. McEwen, *Polymer*, **34**, 501 (1993).
16. M. L. Nelson and R. T. O'Connor, *J. Appl. Polym. Sci.*, **8**, 1311 (1964).
17. J. Marton and H. E. Sparks, *Tappi*, **50**, 363 (1967).
18. J. E. Stone, A. M. Scallan, and P. A. V. Ahlgren, *Tappi*, **54**, 1527 (1971).
19. S. Fukui, D. Tatsumi, and T. Yamauchi, *Nord. Pulp Pap. Res. J.*, **11**, 281 (1996).
20. R. G. J. Miller and H. A. Willis, *Trans. Faraday Soc.*, **49**, 433 (1953).
21. W. C. Sears and W. W. Parkinson Jr., *J. Polym. Sci.*, **21**, 325 (1956).